Korean Journal of Microbiology (2025) Vol. 61, No. 1, pp. 33-45
DOI https://doi.org/10.7845/kjm.2025.4117

eISSN 2383-9902
pISSN 0440-2413

Characterization and expression analysis of fatty acid desaturase genes in Arctic *Chlamydomonas* sp. KNM0029C§

Jeongha So[1,3], Sanghee Kim[1], Jungeun Lee[1], Hyunsik Chae[1], Kitae Kim[2,3], and Sung Mi Cho[1,3]*

[1]*Division of Life Sciences, Korea Polar Research Institute, Incheon 21990, Republic of Korea*
[2]*Division of Glacier and Earth Sciences, Korea Polar Research Institute, Incheon 21990, Republic of Korea*
[3]*Department of Polar Sciences, University of Science and Technology, Incheon 21990, Republic of Korea*

북극 *Chlamydomonas* sp. KNM0029C 지방산 불포화효소 유전자의 특징과 발현 분석§

소정하[1,3] · 김상희[1] · 이정은[1] · 채현식[1] · 김기태[2,3] · 조성미[1,3]*

[1]극지연구소 생명과학연구본부, [2]극지연구소 빙하지권연구본부, [3]과학기술연합대학원대학교, 극지과학 캠퍼스

(Received December 31, 2024; Revised March 6, 2025; Accepted March 17, 2025)

Fatty acid desaturases (FADs) play a crucial role in the biosynthesis of polyunsaturated fatty acids (PUFAs), which are essential for maintaining membrane fluidity in cold environments. This study characterizes and analyzes the expression patterns of FAD genes in the Arctic *Chlamydomonas* sp. KNM 0029C, a psychrophilic microalga with significant potential for biofuel production. Phylogenetic analysis revealed that KNM 0029C is closely related to *C. priscuii* UWO241 belongs to the *Moewusinia* clade, yet distinct from other polar *Chlamydomonas* species, such as ICE-L in the *Monadinia* clade. Transcriptomic analysis identified four major FAD genes—*FAD5*, *FAD6*, *FAD7*, and *Δ4FAD*—all of which are localized in the chloroplast. Notably, *FAD6* was the only *ω*-6 desaturase detected, as KNM0029C lacks the endoplasmic reticulum-localized *FAD2* gene. Protein sequence analysis revealed that *Chlamydomonas* in *Moewusinia* clade (KNM0029C and UWO 241) exhibit protein sequence distances five times greater than those within Chlorophycean/Trebouxiophycean algae. Expression analysis under variable temperature conditions demonstrated a significant up-regulation of all FAD genes at temperature decrease (8°C to 4°C), indicating their role in PUFA synthesis under cold stress. Interestingly, *FAD5* and *FAD7* exhibited increased expression at temperature increase (8°C to 12°C), suggesting a distinct regulatory mechanism for temperature adaptation. These findings highlight the unique genetic variations of KNM0029C in the *Moewusinia* clade from cold environments and indicate its possibility for improving biofuel production by applying genetic engineering tools.

Keywords: polar *Chlamydomonas*, *ω*-6 desaturase, fatty acid desaturase, genetic variation

Microalgae lipids, essential components of cellular and organelle membranes, account for a substantial portion of dry weight, ranging from 5% to 60% (Ben-Amotz et al., 1985). They fulfill two primary functions: serving as storage lipids, predominantly in the form of triacylglycerol (TAG), and acting as structural lipids, specifically glycerophospholipids. Fatty acids (FAs) are essential components that serve as building blocks for lipids (Klok et al., 2014). Microalgal FAs have longer carbon chains and exhibit a greater diversity in the number and positions of double bonds, rendering them more valuable than their plant counterparts (Sawangkeaw and Ngamprasertsith, 2013). The storage TAG, which consists of

***For correspondence.** E-mail: smcho@kopri.re.kr;
Tel.: +82-32-760-5970; Fax: +82-32-760-5509
§Supplemental material for this article may be found at http://www.kjom.org/main.html

three FAs attached to a glycerol backbone (Ördög et al., 2016), found in microalgae, rich in saturated fatty acids (SFAs) and monounsaturated fatty acids (MUFAs), is a valuable resource for transportation biofuels (Breuer et al., 2013; Shen et al., 2016).

Most industrial algal strains are mesophilic, thriving in temperatures ranging from 20°C to 30°C, which enhances their biomass and lipid content (Morales et al., 2021). However, at elevated temperatures, these strains typically produce a higher proportion of SFAs (Sayegh and Montagnes, 2011; Sibi et al., 2016). To improve the ratio of unsaturated fatty acids (UFAs) to SFAs, it is necessary to cultivate these strains at lower temperatures (Olofsson et al., 2012; Sibi et al., 2016) or in nitrogen deprivation conditions (Collet et al., 2014; Griffiths et al., 2012). Unfortunately, this often leads to a reduction in overall biomass (Griffiths et al., 2014). Therefore, it is crucial to identify suitable strains that can sustain high biomass levels while producing polyunsaturated fatty acids (PUFAs) (Schulze et al., 2019). In this context, psychrophilic algae are particularly noteworthy. Psychrophilic algae are defined as organisms with an optimal growth temperature of less than 15°C (Eddy, 1960) and are consistently exposed to low temperatures and icy environments. This persistent cold exposure necessitates the effective regulation of membrane fluidity as a vital defense mechanism (He et al., 2019; Zhang et al., 2020, 2021a).

Despite their notable physiological and industrial potential, research on the lipid profiling and regulatory mechanisms of FA desaturation in psychrophilic algae remains insufficient. Among these, the genus *Chlamydomonas* is the most extensively studied. *C. priscuii* UWO241 and *Chlamydomonas* sp. ICE-L are the representative species of the *Moewusinia* and *Monadinia* clades, respectively. Genomic studies of these species have provided insights into large genome sizes attributed to gene duplications, which support their psychrophilic adaptation (Zhang et al., 2020, 2021a). In contrast, lipid profiling studies have been conducted on the KNM 0029C and RCC2488 strains, both of which have been identified as promising algal candidates as a result of their higher PUFA and carbohydrate contents, making them suitable for biodiesel and bioethanol production (Kim et al., 2020; Morales-Sánchez et al., 2020). Although the lipid composition of these species has been characterized, the underlying genetic regulatory mechanisms governing these processes remain inadequately understood.

Fatty acid desaturase (FAD) is a key enzyme involved in the production of diverse PUFA forms and in increasing PUFA content (Li-Beisson et al., 2015; Nachtschatt et al., 2020). The gene composition of this pathway varies among different organisms (Li-Beisson et al., 2015; Liu et al., 2019). To gain insights into the regulatory mechanisms governing unsaturated fatty acid (UFA) production at low temperatures in psychrophilic algae, we conducted a phylogenetic analysis and performed RNA sequencing of KNM0029C. Based on these data, we characterized the protein features of FADs and compared the characteristics of FAD genes in *Chlamydomonas* sp. KNM0029C with those in *Chlamydomonas* sp. ICE-L, *C. priscuii* UWO241, and the mesophilic species *C. reinhardtii*. Additionally, we analyzed the expression levels of four newly identified FAD genes in *Chlamydomonas* sp. KNM0029C in response to temperature changes. These findings emphasize the importance of psychrophilic algae in identifying species capable of thriving in extreme conditions while producing significant quantities of biofuel.

Materials and Methods

18S Phylogeny

The Arctic *Chlamydomonas* sp. KNM0029C was sourced from the Korea Polar Research Institute Culture Collection for Polar Microorganisms (KCCPM, Korea) and maintained at 8°C in BBM media under constant white light (40 μmol/m^2/s). Cells in the logarithmic growth phase were harvested and homogenized in liquid nitrogen using a mortar and pestle. DNA extraction was performed using the Exgene Plant SV kit (GeneAll, Korea) following the manufacturer's guidelines. The 18S ribosomal RNA sequences, 1,780 bp in length, were amplified via PCR using the 18S JO2 (5'-ACC TGG TTG ATC CTG CCA G-3') and SS17HR (5'-CCT TGT TAC GAC TTC TCC TTC CTC T-3') primers (Verbruggen et al., 2009) with ExTaq polymerase (TaKaRa, Japan). Sequencing was conducted at CosmoGentech (Korea), and the resulting sequences were deposited in the NCBI database (accession

number: PQ645171).

To construct the 18S phylogenetic tree, a total of 40 sequences were retrieved from the NCBI database, including eight *Chlamydomonas* sequences from the Antarctic and Arctic regions: *Chlamydomonas priscuii* UWO241 from Lake Bonney, Antarctica (KP313859); *Chlamydomonas* sp. ICE-W and ICE-L from sea ice near Zhongshan Station, East Antarctica (AY731083 and AY731082); *Chlamydomonas* sp. SAG75.94 from a cold lake in Antarctica (AF514399); *Chlamydomonas* sp. Antarctic 2E9 from Antarctica (AB 001374); *C. malina* RCC2488 from seawater in the Beaufort Sea, Alaska (JN934686); and *Chlamydomonas* sp. ARC from sea ice in the Chukchi Sea, Alaska (EF537906). Multiple sequence alignments were performed using the MAFFT version 7 webserver with default parameters (Katoh et al., 2019). A maximum likelihood (ML) phylogenetic tree was generated using a 1,709-nucleotide dataset of 41 taxa, with the TN93 + R + F model selected based on the Bayesian Information Criterion (BIC). The ML analysis was conducted with 1,000 bootstrap replicates using the PhyML 3.0 webserver (Guindon et al., 2010). Tree visualization was performed using FigTree version 1.4.4 (Rambaut, 2018).

Transcriptome sequencing and de novo assembly

Cells were cultured at 8°C under constant white light (40 μ mol/m^2/s) with shaking until reaching the saturated phase. The cultures were then inoculated into the three different media—sterilized seawater supplemented with F/2 vitamins, BBM, and TAP—and maintained at 8°C for 7 days. Total RNA was isolated using the RNeasy Plant Mini Kit (Qiagen, Germany) in conjunction with the RNase-Free DNase Set (Qiagen, Germany), following the manufacturer's instructions. RNA libraries were constructed using the TruSeq RNA Sample Preparation Kit v2 (Illumina, USA). The libraries were multiplexed at equal ratios, and sequencing was performed using a single lane of the NextSeq Sequencer system (Illumina) in paired-end mode (101 × 2). A total of 12,754,670,341 nucleotides and 95,453,218 raw reads were obtained. The transcriptome data were deposited in GenBank SRA (SRX1165695), and the sequencing data were assigned accession number SRR2189233.

Raw reads were trimmed, filtered, and assembled using CLC Genomics Workbench 7.5 (CLC Bio, Denmark). A total of 14,736 contigs were generated, with an N50 value of 1,019 bp. Of these, 8,947 assembled contigs, representing 60.7% of the dataset, were subjected to a BLASTX search against the NCBI non-redundant protein database (Altschul et al., 1990) using an E-value threshold of 1×10^{-3}. The annotated genes obtained from this analysis were used to identify FADs (Table S1).

Identification of FAD proteins

To identify FAD proteins from the transcriptome data of KNM0029C, a BLASTX search was conducted utilizing ten protein sequences from *C. reinhardtii* (Li-Beisson et al., 2015) as queries. The search was conducted in the local BLAST of BioEdit version 7.2.5, applying an E-value cutoff of 1×10^{-3}. FAD protein sequences from KNM0029C were selected based on the results of the BLAST analysis, focusing on those that matched over 80% of the previously identified protein sequences. Subcellular localization was analyzed using the plant option in TargetP 2.0 (Almagro Armenteros et al., 2019). The protein sequences were validated through Sanger sequencing, with gene-specific primers amplified from the cDNA of KNM0029C (Table S2). These sequences have been deposited in NCBI (accession; PQ634669-PQ 634672).

The domain structure was predicted from the translated contig sequences using the normal mode of the SMART webserver (Letunic et al., 2006). To compare domain sequences, multiple alignments were performed with sequences from *C. priscuii* UWO241, *Chlamydomonas* sp. ICE-L, *C. reinhardtii*, and *Chromochloris zofingiensis* using the MAFFT web server with default settings (Katoh et al., 2019). Following alignment, three H-boxes were designated based on a recent study on FADs in *Chromochloris zofingiensis* (Wu et al., 2021).

Comparison of genetic variation in FAD proteins

To construct the phylogenetic tree for FAD proteins, 53 homologous sequences from 10 representative species were retrieved from the NCBI database: *Arabidopsis thaliana, Brassica napus, Chlamydomonas* sp. ICE-L, *C. priscuii* UWO 241, *C. reinhardtii, Chlorella sorokiniana*, *Chromochloris*

zofingiensis, *Dunaliella salina*, *Glycine max*, and *Haematococcus pluvialis*. These sequences formed the basis for the phylogenetic analysis of FAD proteins. During multiple sequence alignment, CrFAD6a (PNW82666) from *C. reinhardtii* was excluded from phylogenetic tree construction as a result of significant sequence variations. Multiple sequence alignments were conducted using the MAFFT version 7 webserver with default parameters (Katoh et al., 2019). An ML phylogenetic tree was generated using a dataset of 933 amino acids from 57 taxa, with the Q.pfam + G + I model selected based on the BIC. The ML analysis was conducted with 1,000 bootstrap replicates using the PhyML 3.0 webserver (Guindon et al., 2010). Tree visualization was accomplished using FigTree version 1.4.4 (Rambaut, 2018).

Protein sequence distances among FADs were calculated using PROTDIST version 3.5c within BioEdit version 7.2.5. This analysis encompassed twelve Chlorophyceae and two Trebouxiophyceae species, with their corresponding NCBI accession details listed in Table S3. The distances for each pair of species were estimated using the JTT matrix model. Consequently, the distances of each FAD protein in relation to those of KNM0029C were presented.

RT-qPCR analysis

Arctic *Chlamydomonas* sp. KNM0029C was cultured in 20 ml of 3N BBM medium at 8°C, with subsequent transfers to growth chambers set at 4°C and 12°C. After 1, 3, and 7 days of transfer, cells were harvested, frozen in liquid nitrogen, and homogenized using the Tissue Lyser II (QIAGEN, Germany) with stainless steel beads. Total RNA was extracted following the manufacturer's instructions using the RNeasy Plant Mini Kit (QIAGEN, Germany) in conjunction with the RNAase-free DNase set (QIAGEN, Germany).

The cDNA synthesis was performed on 2 μg of total RNA using the TOPscript^{TM} cDNA Synthesis Kit (Enzynomics, Korea). Gene-specific primers, listed in Table S4, were designed, and the amplification efficiency of each primer was tested. To assess the expression stability of reference genes, five candidate reference genes (*actin*, *tubA*, *EF1a*, *rbcL*, and *GAPDH*) were evaluated using RefFinder (Chen et al., 2019). Among these, *actin* and *EF1a* were identified as the most stable genes based on a comprehensive comparison of major computational programs, including geNorm, BestKeeper, NormFinder, and the delta-CT method, using CT values from all cDNA samples (Table S5). The arithmetic-geometric mean of CT values from the two reference genes was used to calculate expression levels. RT-qPCR analysis was conducted using biological triplicates. Gene expression levels were calculated using the delta-delta CT method (Livak and Schmittgen, 2001), with the expression level at 0 days set as the control (assigned a value of 1). A normality test was performed using SPSS version 21. If normality was satisfied, a one-way ANOVA was conducted. For post-hoc analysis, Turkey's method was applied when equal variance was met, whereas Dunnett's method was used when equal variance was not assumed.

Results

Phylogenetic position of Arctic *Chlamydomonas* sp. KNM0029C

In the 18S phylogenetic analysis, *Chlamydomonas* sp. KNM0029C was classified within the *Moewusinia*-clade (Fig. 1), one of the polyphyletic clades of the genus *Chlamydomonas* (Lemieux et al., 2015; Pröschold et al., 2001). KNM0029C exhibited a sister relationship with an uncultured Chlorophyta species isolated from seawater in Finland. This clade was closely related to three polar species: *C. malina* RCC2488 from the Arctic region, as well as *C. priscuii* UWO 241 and *Chlamdyomonas* sp. SAG75.94 from Antarctica. The remaining four *Chlamydomonas* species, including *Chlamydomonas* sp. ICE-L, were placed within the *Monadinia* clade, where they clustered alongside two *Microglena* species isolated from the Arctic region. Meanwhile, the mesophilic *C. reinhardtii* was classified within the *Reinhardtinia* clade. Each clade comprised bipolar species inhabiting diverse ecological environments, a trend frequently observed in polar microalgal lineages (Segawa et al., 2018; Uhlig et al., 2015). Based on these findings, KNM0029C and UWO241, both within the *Moewusinia* clade, were compared to ICE-L of the *Monadinia* clade and *C. reinhradtii* of the *Reinhardtinia* clade to assess the genetic diversity of FAD genes in relation to phylogeny.

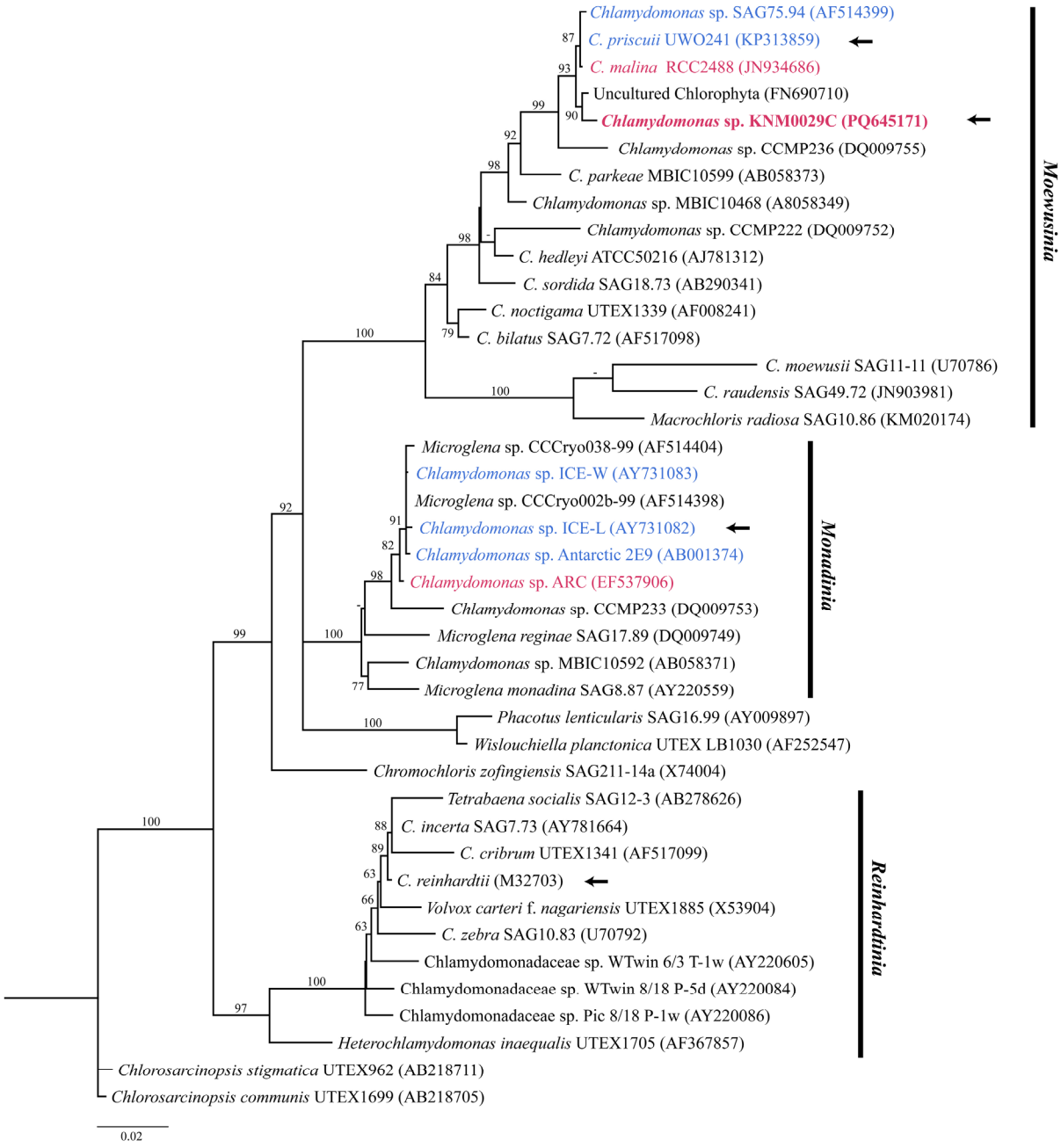

Fig. 1. Maximum-likelihood phylogeny of 18S sequences from the genus *Chlamydomonas* and its relative. Eight taxa from the Arctic and Antarctic regions are marked with pink and blue characters, respectively. The phylogenetic tree distinguishes three clades: *Moewusinia*, *Monadinia*, and *Reinhardtinia*. Three polar *Chlamydomonas* species and the non-polar *C. reinhardtii* are indicated with black arrows. The numbers on the branches indicate a bootstrap value (> 0.5).

Identification of FAD genes

Through BLASTX analysis, we identified seven putative FAD proteins based on sequence homology with *C. reinhardtii* (Table S6): FAD6 (*ω*-6 fatty acid desaturase), FAD6-like, FAD7 (chloroplast glycerolipid *ω*-3 fatty acid desaturase), FAD4 (Δ-3 palmitate desaturase), FAD5 (Monogalactosyldiacylglycerol (MGDG)-specific palmitate Δ-7 desaturase), FAD5-like, and Δ4FAD (MGDG-specific Δ-4 fatty acid desaturase). No homologous sequences were found for FAD2 (*ω*-6 fatty acid desaturase, Δ-12) or CrDES (a front-end *ω*-13

Table 1. Newly identified FAD proteins of *Chlamydomonas* sp. KNM0029C and their homologs from four representative species with available genomes: UWO241 (Zhang et al., 2021a), ICE-L (Zhang et al., 2020), Cr (Li-Beisson et al., 2015), and Cz (Zhang et al., 2021b)

Gene	KNM0029C*	UWO241	ICE-L	Cr	Cz
FAD2	n.d.	n.d.	n.d.	PNW70229	QWW89551
FAD4	(2)	KAG1665443	n.d.	PNW72323	QWW89561
FAD5	PQ634669	KAG1658363	ANF04697	PNW78440	QWW89556
FAD5-like	(2)	n.d.	n.d.	PNW83842 PNW83836	QWW89557 QWW89558
FAD6	PQ634670	KAG1669387	AEK76074	PNW74228	QWW89552
FAD6-like	(2)	n.d.	n.d.	PNW82666	QWW89553
FAD7	PQ634671	KAG1662017	ACX42440 AGF90969	PNW88647	QWW89554 QWW89555
Δ4FAD	PQ634672	n.d.	AFO64943	PNW88628	QWW89559 QWW89560
DES	n.d.	n.d.	n.d.	PNW77828-9	n.d.
Total	4	4	5	10	11

* Number of parentheses indicated the incomplete contig sequences. They were excluded the total number of FADs.

desaturase), both of which are localized in the endoplasmic reticulum (ER). Domain structure prediction revealed that FAD6-like, FAD4, and FAD5-like proteins were incomplete structures because of short sequence lengths, which is less than 80% of coverage compared to corresponding sequences of *C. reinhardtii*, and thus they were excluded in the further analysis. The remaining FAD6, FAD7, FAD5, and Δ4FAD proteins indicated that all had the FA_desaturase domain (Pfam: PF00487) along with several transmembrane (TM) domains (Fig. S1). Subcellular localization analysis using TargetP predicted that these proteins were localized in the chloroplast, suggesting they are likely membrane-embedded proteins in this organelle. In addition, FAD7 (contig06462) and Δ4FAD (contig03537) exhibited additional functional domains at the N-terminus: FAD7 contained a DUF3474 domain (domain of unknown function 3474; Pfam: PF11960), whereas Δ4FAD possessed a Cyt-b5 domain (cytochrome b5-like heme/steroid-binding domain; Pfam: PF00173). These domain structure characteristics were highly consistent with those observed in *C. priscuii* UWO241, *Chlamydomonas* sp. ICE-L, *C. reinhardtii*, and *Chromochloris zofingiensis* (Fig. S1). These findings were validated through Sanger sequencing, and the resulting sequences were deposited in the NCBI database (Table 1). In total, we identified four FAD genes: *FAD5* (PQ634669), *FAD6* (PQ634670), *FAD7* (PQ 634671), and *Δ4FAD* (PQ634672). The whole genome of KNM0029C is necessary to validate that KNM0029C possesses only four, which is half the number found in *C. reinhardtii*. However, this reduction of FADs was similarly observed for the genomes of *C. priscuii* UWO241 and *Chlamydomonas* sp. ICE-L. Although the three polar *Chlamydomonas* species—KNM0029C, UWO241, and ICE-L—differ in their FAD protein composition, they all lack homologous sequences for FAD2 and CrDES.

Comparison of histidine boxes

The histidine box (H-box) of FAD proteins is related to the integral ability to bind iron ions for making desaturation bonds of FAs. The structure of these H-boxes is highly conserved, comprising $H(X)_{3-4}H$, $H(X)_{2-3}HH$, and $H/Q(X)_{1-2}HH$ (Nachtschatt et al., 2020). Multiple alignments of the domain sequences confirm that all proteins maintain these three H-boxes, suggesting they likely exhibit general desaturase activity (Figs. 2 and S2). The sequences of the H-boxes are predominantly conserved. The Δ4FAD retains all conserved H-box sequences, whereas FAD5 and FAD7 display fixed histidine residues with minor substitutions in the middle positions (Fig. S2): M^{188}, S^{190} in H-box I, Y^{225} in H-box II, and N^{357} in H-box III for CrFAD5 (PNW78440); T^{167} in H-box II and V^{337} in H-box III for CrFAD7 (PNW88647). Notably, the sequences of H-boxes for FAD6 exhibit the most significant substitutions (Fig. 2). Thirteen of all 15 amino acids are

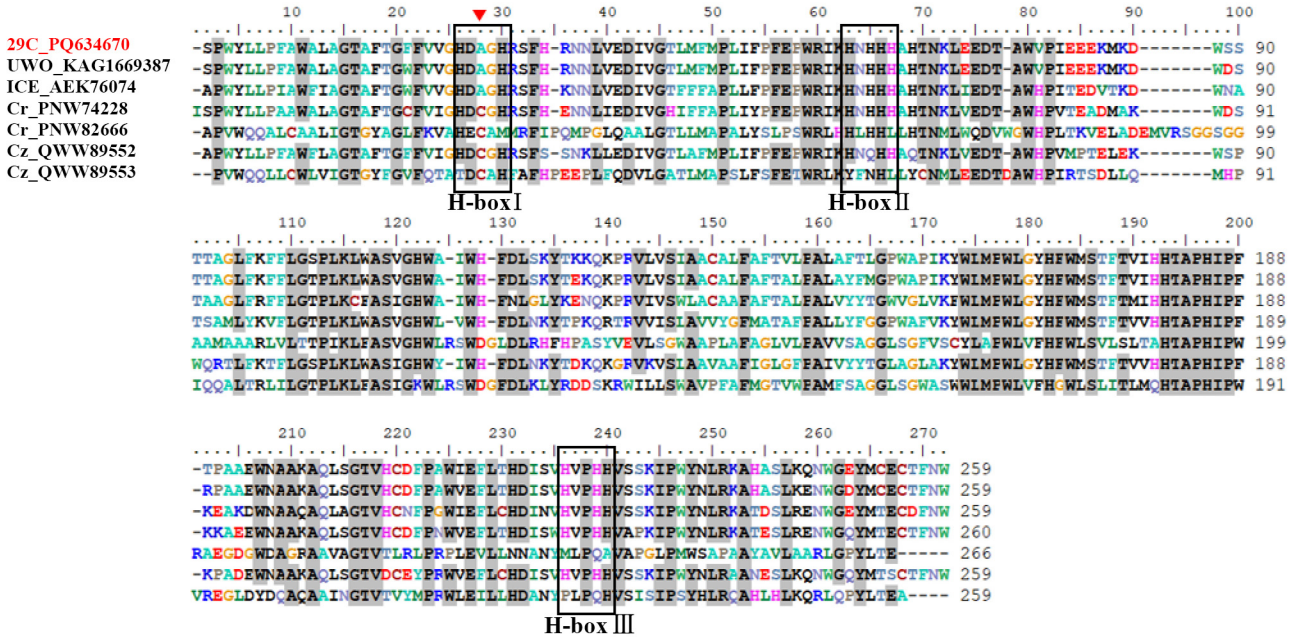

Fig. 2. Multiple alignments of FA_desaturase domain (Pfam: PF00487) of FAD6 proteins. Three H-boxes are marked with black boxes. The red arrowhead indicates the C-to-A substitution in H-box I. The grey block indicates the highly conserved sequences. Prefix means an abbreviation of species name: 29C, *Chlamydomonas* sp. KNM0029C; UWO, *C. priscuii* UWO241; ICE, *Chlamydomonas* sp. ICE-L; Cr, *C. reinhardtii*; Cz, *Chromochloris zofingiensis*.

variable except H^{185} in H-box II and P^{346} in H-box III for CrFAD6 (PNW74228). Among these, a C^{148} in H-box I found in non-polar species like *C. reinhardtii* and *Chromochloris zofingiensis* while it substituted to A is distinctly identified in polar *Chlamydomonas* (KNM0029C, UWO241, and ICE-L). This variation in the H-boxes of FAD6 represents a remarkable characteristic when compared to other FADs, and it is necessary to validate the impact of this substitution on the flexibility of iron-bound moiety of psychrophilic algal FAD6.

Genetic variations of FADs

The phylogenetic analysis of FAD proteins revealed that the four FADs of KNM0029C grouped monophyletically into the subfamilies of FAD5, FAD6, FAD7, and Δ4FAD clades (Fig. 3). Within each subfamily, FAD5, FAD6, and FAD7 of KNM0029C exhibited a sister relationship with those of UWO241, demonstrating perfect support, whereas the FADs of ICE-L were positioned further away. Although FAD6, FAD7, and Δ4FAD of ICE-L were closely associated with the KNM0029C/UWO241 clade, this association had a low support value (Fig. 3).

The phylogenetic relationship was further substantiated by PROTDIST analysis, which estimated amino acid substitutions at each site between KNM0029C and various other species utilizing a matrix model (Table S7 and Fig. 4). Noteworthy findings indicated that the FADs of UWO241 exhibited the lowest substitution values, all of which were below 0.2. In contrast, the FADs from ICE-L were significantly distanced from KNM0029C, with substitution values ranging from 0.87 to 1.10. In the analysis of non-polar species (excluding UWO241 and ICE-L), the distance values among all FAD proteins ranged from 0.21 to 0.46, demonstrating no significant differences even with the inclusion of Trebouxiophycean algae. This finding suggests that FAD proteins have maintained relative stability at the class level. In detail, FAD6 and FAD7, which are responsible for the sequential biosynthesis of UFAs, exhibited moderate variations, with differences measured at 0.31 and 0.21, respectively. Conversely, FAD5 displayed a higher degree of variation at 0.46 within the Chlorophyceae/Trebouxiophyceae group. Collectively, these results imply that the FADs in the polar *Chlamydomonas* in *Moewusinia* clade have undergone an independent evolutionary trajectory when compared to the green algal lineages.

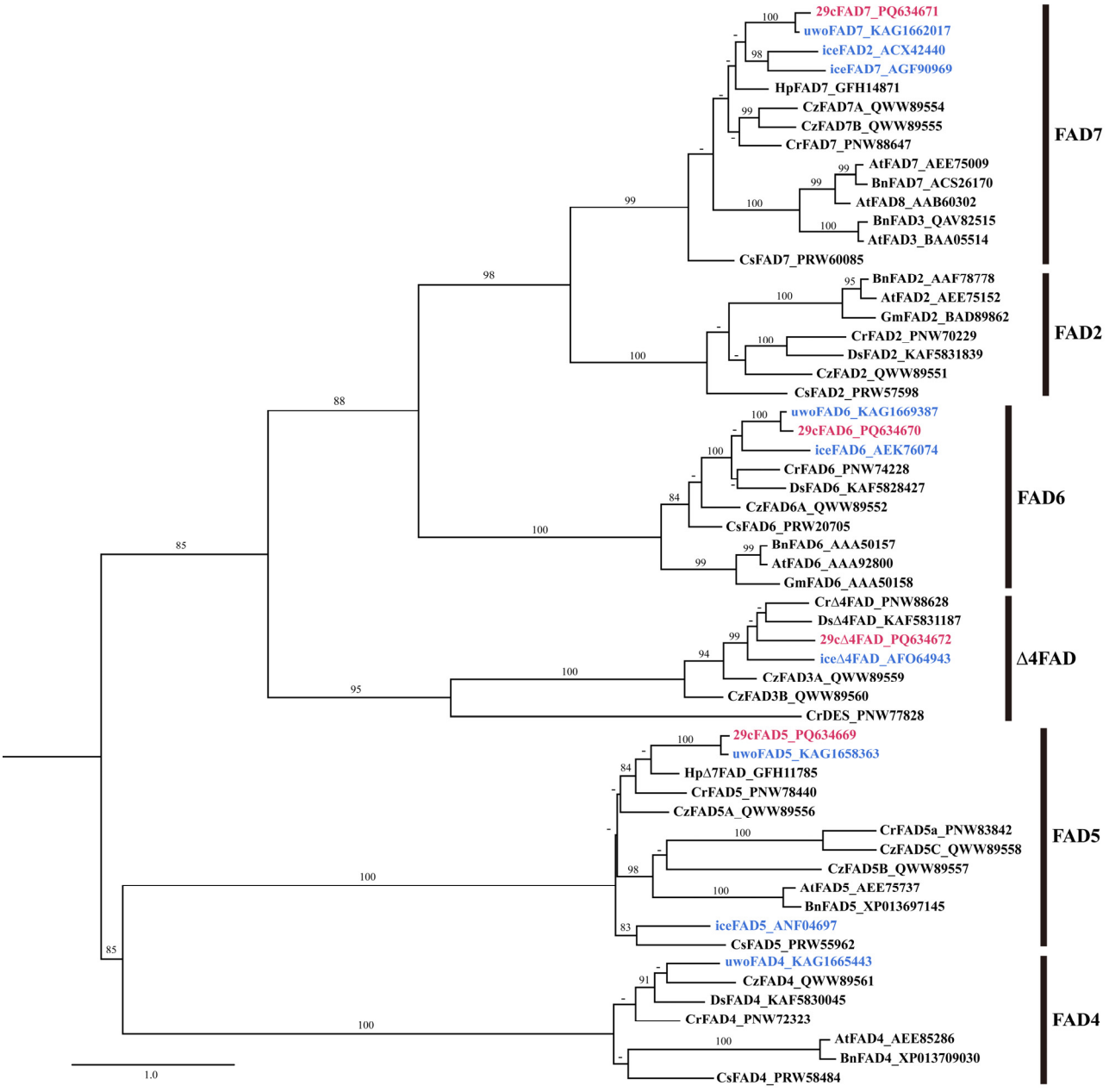

Fig. 3. Maximum-likelihood phylogeny of FAD proteins from algae and plants. Pink and blue characters indicate the proteins of species from the Arctic and Antarctic regions, respectively. Six subclades of FAD proteins were designated according to the annotation of *C. reinhardtii* (Li-Beisson et al., 2015). The numbers on the branches indicate a bootstrap value (> 0.5). In addition to prefix information of Fig. 2, five taxa were added: At, *Arabidopsis thaliana*; Bn, *Brasicca napus*; Cs, *Chlorella sorokiniana*; Ds, *Dunaliella salina*; Hp, *Haematococcus pluvialis*.

Gene expression of FADs in response to temperature changes

In this study, we investigated the expression of four FAD genes in KNM0029C under varying temperature conditions, specifically assessing their responses to an increase to 12°C and a decrease to 4°C, with 8°C serving as the control. Overall, the expression levels of all genes were up-regulated at 4°C, although their responses varied at 12°C (Fig. 5). Notably, *FAD6* expression increased drastically, reaching a 3-fold up-regulation on the first day at 4°C, after which it gradually declined to 1.7-fold by day 7. However, at 12°C, *FAD6* exhibited slight suppression throughout the 7-day

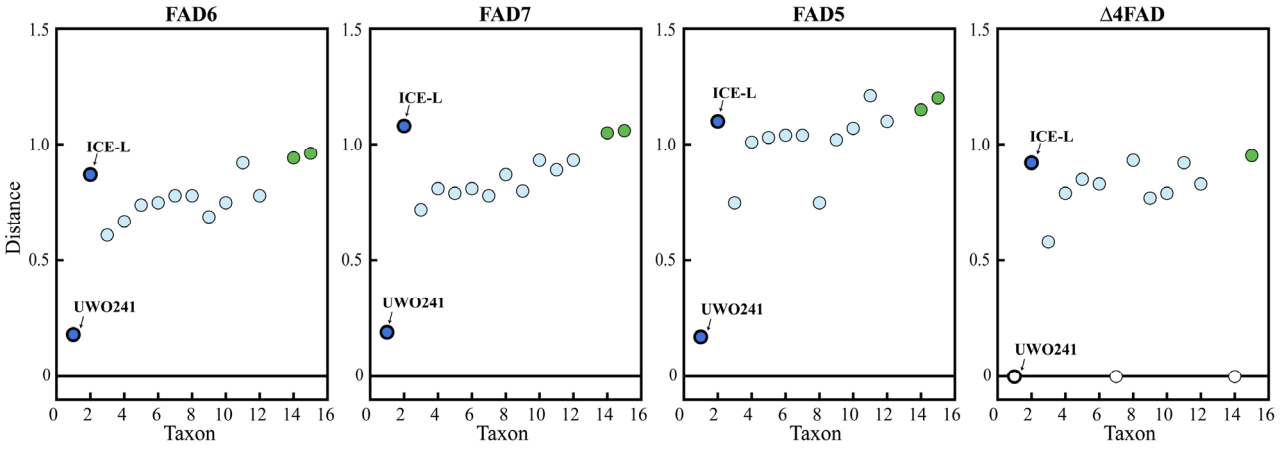

Fig. 4. Pairwise protein distance by PROTDIST analysis. Pairwise distances were estimated with proteins between KNM0029C and others based on the JTT model. Blue, light blue and green indicate polar *Chlamydomonas*, other Chlorophyceae and Trebouxiophyceae taxa, respectively. The detailed information of taxa is listed in Tables S3 and S7.

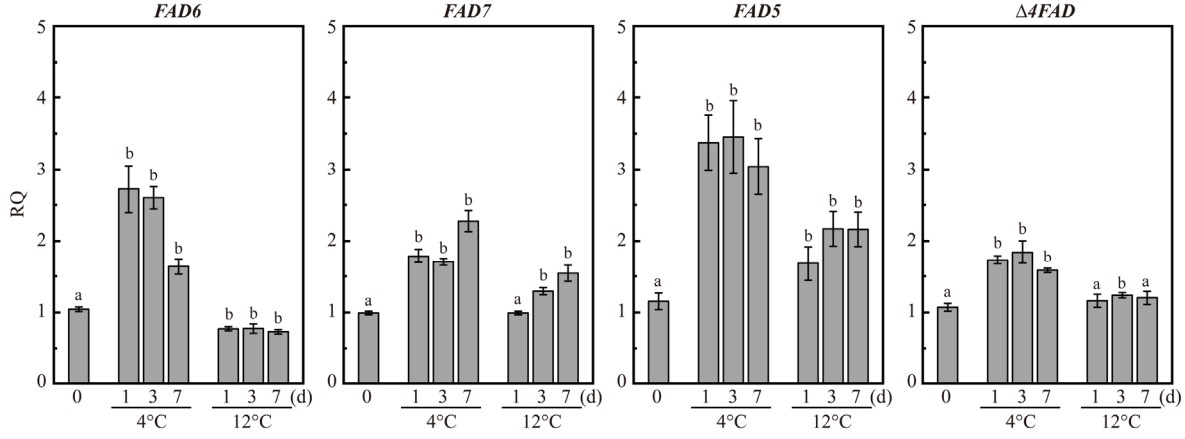

Fig. 5. Gene expression pattern of four FAD genes of KNM0029C in response to temperature changes using RT-qPCR. *Actin* and *EF1a* were used as reference genes. The expression level of a gene at 0 days was assigned a value of 1 as a control. Data represent the means ± standard deviation (SD) for three biological replicates.

period. In contrast, *FAD7* demonstrated a substantial increase, reaching up to 2.2-fold on day 7, with a consistent upward trend at 4°C over the 7-day period, although remaining below 2-fold. *FAD5* showed strong up-regulation, peaking at 3.2-fold on the first day at 4°C and maintaining this elevated expression level for 7 days. Interestingly, *FAD5* expression also increased at 12°C, though to a lesser extent than at 4°C and remained unchanged at 12°C. These expression patterns can be categorized into two distinct groups: (1) *FAD6* and *Δ4FAD*, which are primarily induced by low temperatures, and (2) *FAD5* and *FAD7*, which are influenced by temperature fluctuations.

Discussion

A single ω-6 desaturase system in polar *Chlamydomonas*: The absence of FAD2

In comparison to the FAD genes of *C. reinhardtii*, polar *Chlamydomonas* exhibits a reduced number of FAD genes, notably lacking the homologous CrFAD2 and CrDES proteins (Table 1). CrDES has been identified as an ω-13 desaturase responsible for the ω-9 unsaturated C18/C20 FAs and is associated with the synthesis of 18:3 $\Delta^{5,9,12}$ (pinolenic acid) and 18:4 $\Delta^{5,9,12,15}$ (coniferonic acid), which are atypical FAs found in algae (Kajikawa et al., 2006). No homologs of

CrDES have been identified in algae, and this also holds true for polar *Chlamydomonas*.

The absence of FAD2 is particularly significant, as it is generally present in most algal species (Wu et al., 2021). FAD2 and FAD6 function as ω-6 desaturases located in the ER and chloroplast, respectively, utilizing different electron donor systems: NADP for FAD2 and ferredoxin for FAD6 (Chi et al., 2008). Consequently, FAD6 cannot operate in the ER like FAD2. Although the absence of FAD2 suggests an impact on PUFA production, KNM0029C demonstrated that this alga produced approximately three times more PUFAs than *C. reinhardtii* under low-temperature conditions (Kim et al., 2016). This finding supports the idea that chloroplastic FAD6 may play a more significant role as the ω-6 desaturase compared to ER-localized FAD2, particularly since microalgae typically contain large chloroplasts, which occupy approximately 70% of the cellular volume (Harris, 2001; Zhang et al., 2021b).

Although a functional study is required to assess the benefits of a simple ω-6 desaturase system in polar *Chlamydomonas*, FAD6 may serve as a precise regulator of the ratio between MUFA and PUFA production in response to decreasing temperatures in KNM0029C. As FAD6 is the initial enzyme responsible for PUFA synthesis, its induction —particularly under decreasing temperature conditions— suggests a critical regulatory role compared to other FAD genes. This regulation is likely to influence total PUFA levels under low-temperature conditions (Fig. 5). Consequently, it is reported that KNM0029C produced higher PUFA concentrations at 4°C compared to 12°C (Kim et al., 2016). In contrast, another study indicates that FAD7 can act as a limiting enzyme in the regulation of PUFA production in *Chlamydomonas* sp. ICE-L (An et al., 2013). Therefore, it should be further examined the regulatory roles of chloroplastic FAD genes under the low-temperature conditions of microalgae especially in polar microalgae.

Various responses of FAD genes to temperature condition

Temperature is a crucial factor influencing lipid productivity and FA composition in algae. Typically, in response to low temperatures, most algae increase the ratio of UFAs to SFAs to enhance membrane flexibility, although this adaptation often results in decreased biomass productivity (Ho et al., 2014; Ördög et al., 2016). In contrast, psychrophilic algae thrive in low-temperature environments while maintaining elevated levels of UFAs. Although some low-temperature responses have been elucidated (An et al., 2013), the regulatory mechanisms underlying lipid profile changes remain unclear.

In this study, we identified two distinct expression patterns of FAD genes in KNM0029C in response to temperature changes. Upon a temperature decrease from 8°C to 4°C, all four FAD genes were up-regulated, leading to enhanced PUFA accumulation, a phenomenon commonly observed in other algae. Interestingly, we found that KNM0029C tightly regulates PUFA levels at the transcriptional level in response to a temperature increase of 4°C. Specifically, when KNM 0029C cells were transferred from 8°C to 12°C, *FAD5* and *FAD7* expression was up-regulated. The *FAD5* gene encodes the first desaturation enzyme that acts on C16 FA in MGDG molecules, which are the most abundant glycerolipids in *C. reinhardtii* (Li-Beisson et al., 2015). Although the precise function of *FAD5* in algae remains unclear, its up-regulation may contribute to the accumulation of MUFAs in the cell. In this context, the suppression of *FAD6* plays a crucial role, as this enzyme is involved in the biosynthesis of C18:2 and C16:2 FAs, which are key components of a wide range of PUFAs. Therefore, the combined expression *FAD5* and *FAD6* forms a major regulatory module for MUFA accumulation under a temperature increase of 4°C. Although *FAD7* up-regulation is associated with increased C18:3 and C16:3 PUFA levels, its impact is likely minor since its substrates, C18:2 and C16:2, are produced by *FAD6*. Additionally, *Δ4FAD*, an enzyme responsible for the production of C16:3 and C16:4 PUFAs, remained unchanged under elevated temperature conditions. Taken together, these findings emphasize that PUFA production in polar microalgae is finely regulated through the precise modulation of FAD gene expression in response to fluctuating environmental temperatures.

Promising algal strains for biofuel production: *Chlamydomonas–Moewusinia* clade

The gene family of FADs is a well-conserved system in green lineages (Fig. S3), with each subfamily sharing essential residues in three H-boxes. However, the overall sequence similarity varies significantly. The FADs of KNM 0029C closely resemble those of UWO241 while showing minimal similarity to those of ICE-L despite all three being found in cold and saline environments. The differences in FADs between KNM0029C/UWO241 and other algal strains are striking, with a divergence five times greater than that observed between Chlorophyceae and Trebouxiophyceae algae (Fig. 4). Rather than being linked to ecological conditions, these differences appear to correlate with species lineage; KNM0029C and UWO241 belong to *Chlamydomonas-Moewusinia* clade, whereas ICE-L is *Chlamdyomonas-Monadinia* clade (Fig. 1).

Recently, an Arctic strain of *C. marina* RCC2488 in the *Moewusinia* clade was reported to possess high protein PUFA content when cultivated at 8°C (Schulze et al., 2019). This alga has demonstrated substantial biomass and PUFA production across a wide range of salinities (0 to 35 ppt) and light intensities (70−500 µmol/m²/s), indicating its potential as a promising strain under 8°C conditions (Morales-Sánchez et al., 2020). Likewise, KNM0029C exhibited higher biomass in freshwater Bold's Basal Medium (BBM) and Tris-acetate-phosphate (TAP) media compared to marine F/2 medium at 8°C (Kim et al., 2016). This alga has also been validated as a viable candidate for a co-production strategy aimed at generating biodiesel and bioethanol as a result of its significant carbohydrate content (Kim et al., 2020). In terms of physiological responses, the genetic composition of *C. marina* RCC2488 is anticipated to be similar to that of KNM0029C/UWO241.

FA composition of microalgae is a critical factor in determining the fluidity at low temperatures and oxidative stability of biodiesel. Therefore, it is important to maintain a high concentration of SFAs and MUFAs in microalgal cells for producing high-quality biodiesel. To meet the condition, myriad strategies have been developed (Morales et al., 2021). However, a key conclusion is that FA composition is species-specific (Morales et al., 2021; Morales-Sánchez et al., 2020). Therefore, the discovery of new algal cultures remains essential. Regarding this, the *Chlamydomonas-Moewusinia* clade, KNM0029C, RCC2488, and UWO241, will offer valuable opportunities for leading research on alternative materials for biofuel industries.

Conclusion

This study provides a comprehensive characterization of FAD genes in the Arctic *Chlamydomonas* sp. KNM0029C, elucidating its evolutionary adaptation and lipid metabolism in cold environments. Phylogenetic analysis demonstrated that KNM0029C is closely related to other psychrophilic *Chlamydomonas* species but exhibits a distinct FAD gene composition, notably lacking the ER-localized *FAD2* gene. Expression analysis revealed that all four identified FAD genes were up-regulated at lower temperatures, supporting their role in maintaining membrane fluidity through increased PUFA synthesis. Additionally, the differential expression of *FAD5* and *FAD7* at higher temperatures suggests a complex regulatory mechanism for lipid biosynthesis in response to temperature fluctuations. Given its ability to sustain high biomass and lipid production under low temperatures, KNM0029C emerges as a promising candidate for biofuel applications. The findings from this study not only enhance our understanding of lipid metabolism in psychrophilic algae but also provide valuable insights for biotechnological advancements in sustainable biofuel production.

적 요

지방산 불포화 효소(FADs)는 다중 불포화지방산의 생합성에서 중요한 역할을 하며, 이는 저온 환경에서 막의 유동성을 유지하는데 필수 요소이다. 본 연구는 바이오연료 생산 잠재력을 인정받은 호냉성 미세조류 북극 *Chlamydomonas* sp. KNM0029C의 FAD 유전자의 특성과 발현 패턴을 분석하였다. 계통분류 연구결과 *Chlamydomonas* sp. KNM0029C는 *C. priscuii* UWO241과 매우 가까웠으며 *Moewusinia* 계통군에 속하고, *Chlamydomonas* sp. ICE-L을 포함한 다른 극지 *Chlamydomonas*종이 속하는 *Monadinia* 계통군과 구별되었다. 전사체 분석 결과 4개의 주요 FADs 유전자(*FAD5*, *FAD6*,

FAD7, *Δ4FAD)*가 동정 되었으며, 모두 엽록체에 위치하는 것으로 확인되었다. 특히, *Chlamydomonas* sp. KNM0029C는 소포체에 위치하는 *FAD2* 유전자가 발견되지 않아, 단일 *ω*-6 불포화 효소로 *FAD6*를 갖는 특징이 있었다. 전체 단백질 서열 치환도를 분석한 결과, *Chlamydomonas-Moewusinia*계통군(KNM0029C와 UWO241)의 단백질 서열은 녹조강/트레복시오강 조류와 5배 이상 다른 뚜렷한 차이를 보였다. 온도변화에 따른 FAD 유전자의 발현 분석 결과, 모든 FAD 유전자가 온도 하강 조건(8℃ → 4℃)에서 유의미한 발현 증가를 보였고, 이 결과는 모든 FAD 유전자가 저온 조건의 다중 불포화지방산 합성에 중요한 역할을 하는 것을 시사한다. 흥미롭게도, *FAD5*와 *FAD7*은 온도 상승 조건(8℃ → 12℃)에서 발현이 증가하였는데, 이것은 온도 적응에 대한 개별 조절 메커니즘에 의한 것으로 판단된다. 이러한 연구 결과는 저온 환경의 *Chlamydomonas-Moewusinia*계통군의 *Chlamydomonas* sp. KNM0029C가 갖는 고유한 유전적 변이를 의미하며, 유전공학적 방법을 적용하여 바이오연료 생산을 개선할 수 있는 가능성을 시사한다.

Acknowledgments

This work was supported by a Korea Polar Research Institute (KOPRI) grant funded by the Ministry of Oceans and Fisheries (PE25140).

Conflict of Interest

The authors declare no conflict of interest.

References

Almagro Armenteros JJ, Salvatore M, Emanuelsson O, Winther O, von Heijne G, et al. 2019. Detecting sequence signals in targeting peptides using deep learning. *Life Sci Alliance*. 2: e201900429.

Altschul SF, Gish W, Miller W, Myers EW, Lipman DJ. 1990. Basic local alignment search tool. *J Mol Biol*. 215: 403-410.

An M, Mou S, Zhang X, Ye N, Zheng Z, et al. 2013. Temperature regulates fatty acid desaturases at a transcriptional level and modulates the fatty acid profile in the Antarctic microalga *Chlamydomonas* sp. ICE-L. *Bioresour Technol*. 134: 151-157.

Ben-Amotz A, Tornabene TG, Thomas WH. 1985. Chemical profile of selected species of microalgae with emphasis on lipids 1. *J Phycol*. 21: 72-81.

Breuer G, Lamers PP, Martens DE, Draaisma RB, Wijffels RH. 2013. Effect of light intensity, pH, and temperature on triacylglycerol (TAG) accumulation induced by nitrogen starvation in *Scenedesmus obliquus*. *Bioresour Technol*. 143: 1-9.

Chen C, Wu J, Hua Q, Tel-Zur N, Xie F, et al. 2019. Identification of reliable reference genes for quantitative real-time PCR normalization in pitaya. *Plant Methods*. 15: 70.

Chi X, Zhang X, Guan X, Ding L, Li Y, et al. 2008. Fatty acid biosynthesis in eukaryotic photosynthetic microalgae: identification of a microsomal delta 12 desaturase in *Chlamydomonas reinhardtii*. *J Microbiol*. 46: 189-201.

Collet P, Lardon L, Hélias A, Bricout S, Lombaert-Valot I, et al. 2014. Biodiesel from microalgae – Life cycle assessment and recommendations for potential improvements. *Renew Energy*. 71: 525-533.

Eddy BP. 1960. The use and meaning of the term 'psychrophilic'. *J Appl Bacteriol*. 23: 189-190.

Griffiths MJ, van Hille RP, Harrison ST. 2012. Lipid productivity, settling potential and fatty acid profile of 11 microalgal species grown under nitrogen replete and limited conditions. *J Appl Phycol*. 24: 989-1001.

Griffiths MJ, van Hille RP, Harrison ST. 2014. The effect of nitrogen limitation on lipid productivity and cell composition in *Chlorella vulgaris*. *Appl Microbiol Biotechnol*. 98: 2345-2356.

Guindon S, Dufayard JF, Lefort V, Anisimova M, Hordijk W, et al. 2010. New algorithms and methods to estimate maximum-likelihood phylogenies: assessing the performance of PhyML 3.0. *Syst Biol*. 59: 307-321.

Harris EH. 2001. *Chlamydomonas* as a model organism. *Annu Rev Plant Physiol Plant Mol Biol*. 52: 363-406.

He Y, Zheng Z, An M, Chen H, Qu C, et al. 2019. Molecular cloning and functional analysis of a Δ^{12}-fatty acid desaturase from the Antarctic microalga *Chlamydomonas* sp. ICE-L. *3 Biotech*. 9: 328.

Ho SH, Chen CNN, Lai YY, Lu WB, Chang JS. 2014. Exploring the high lipid production potential of a thermotolerant microalga using statistical optimization and semi-continuous cultivation. *Bioresour Technol*. 163: 128-135.

Kajikawa M, Yamato KT, Kohzu Y, Shoji S, Matsui K, et al. 2006. A front-end desaturase from *Chlamydomonas reinhardtii* produces pinolenic and coniferonic acids by *ω*3 desaturation in methylotrophic yeast and tobacco. *Plant Cell Physiol*. 47: 64-73.

Katoh K, Rozewicki J, Yamada KD. 2019. MAFFT online service: multiple sequence alignment, interactive sequence choice and visualization. *Brief Bioinform*. 20: 1160-1166.

Kim EJ, Jung W, Lim S, Kim S, Han SJ, et al. 2016. Growth and lipid content at low temperature of Arctic alga *Chlamydomonas* sp. KNM0029C. *Bioprocess Biosyst Eng*. 39: 151-157.

Kim EJ, Kim S, Choi HG, Han SJ. 2020. Co-production of biodiesel and bioethanol using psychrophilic microalga *Chlamydomonas*

sp. KNM0029C isolated from Arctic sea ice. *Biotechnol Biofuels*. 13: 20.

Klok AJ, Lamers PP, Martens DE, Draaisma RB, Wijffels RH. 2014. Edible oils from microalgae: insights in TAG accumulation. *Trends Biotechnol*. 32: 521–528.

Lemieux C, Vincent AT, Labarre A, Otis C, Turmel M. 2015. Chloroplast phylogenomic analysis of chlorophyte green algae identifies a novel lineage sister to the Sphaeropleales (Chlorophyceae). *BMC Evol Biol*. 15: 264.

Letunic I, Copley RR, Pils B, Pinkert S, Schultz J, et al. 2006. SMART 5: domains in the context of genomes and networks. *Nucleic Acids Res*. 34: D257–260.

Li-Beisson Y, Beisson F, Riekhof W. 2015. Metabolism of acyl-lipids in *Chlamydomonas reinhardtii*. *Plant J*. 82: 504–522.

Liu J, Sun Z, Mao X, Gerken H, Wang X, et al. 2019. Multiomics analysis reveals a distinct mechanism of oleaginousness in the emerging model alga *Chromochloris zofingiensis*. *Plant J*. 98: 1060–1077.

Livak KJ, Schmittgen TD. 2001. Analysis of relative gene expression data using real-time quantitative PCR and the $2^{-\Delta\Delta C}_{T}$ method. *Methods*. 25: 402–408.

Morales M, Aflalo C, Bernard O. 2021. Microalgal lipids: A review of lipids potential and quantification for 95 phytoplankton species. *Biomass Bioenergy*. 150: 106108.

Morales-Sánchez D, Schulze PS, Kiron V, Wijffels RH. 2020. Production of carbohydrates, lipids and polyunsaturated fatty acids (PUFA) by the polar marine microalga *Chlamydomonas malina* RCC2488. *Algal Res*. 50: 102016.

Nachtschatt M, Okada S, Speight R. 2020. Integral membrane fatty acid desaturases: A review of biochemical, structural, and biotechnological advances. *Eur J Lipid Sci Technol*. 122.

Olofsson M, Lamela T, Nilsson E, Bergé JP, Del Pino V, et al. 2012. Seasonal variation of lipids and fatty acids of the microalgae *Nannochloropsis oculata* grown in outdoor large-scale photobioreactors. *Energies*. 5: 1577–1592.

Ördög V, Stirk WA, Bálint P, Aremu AO, Okem A, et al. 2016. Effect of temperature and nitrogen concentration on lipid productivity and fatty acid composition in three *Chlorella* strains. *Algal Res*. 16: 141–149.

Pröschold T, Marin B, Schlösser UG, Melkonian M. 2001. Molecular phylogeny and taxonomic revision of *Chlamydomonas* (Chlorophyta). I. Emendation of *Chlamydomonas* Ehrenberg and *Chloromonas* Gobi, and description of *Oogamochlamys* gen. nov. and *Lobochlamys* gen. nov. *Protist*. 152: 265–300.

Rambaut A. 2018. FigTree v1.4.4. https://github.com/rambaut/figtree/releases/tag/v1.4.4 (last accessed 01 October 2024).

Sawangkeaw R, Ngamprasertsith S. 2013. A review of lipid-based biomasses as feedstocks for biofuels production. *Renew Sustain Energy Rev*. 25: 97–108.

Sayegh FAQ, Montagnes DJS. 2011. Temperature shifts induce intraspecific variation in microalgal production and biochemical composition. *Bioresour Technol.* 102: 3007–3013.

Schulze PS, Hulatt CJ, Morales-Sánchez D, Wijffels RH, Kiron V. 2019. Fatty acids and proteins from marine cold adapted microalgae for biotechnology. *Algal Res.* 42: 101604.

Segawa T, Matsuzaki R, Takeuchi N, Akiyoshi A, Navarro F, et al. 2018. Bipolar dispersal of red-snow algae. *Nat Commun.* 9: 3094.

Shen PL, Wang HT, Pan YF, Meng YY, Wu PC, et al. 2016. Identification of characteristic fatty acids to quantify triacylglycerols in microalgae. *Front Plant Sci.* 7: 162.

Sibi G, Shetty V, Mokashi K. 2016. Enhanced lipid productivity approaches in microalgae as an alternate for fossil fuels – A review. *J Energy Inst.* 89: 330–334.

Uhlig C, Kilpert F, Frickenhaus S, Kegel JU, Krell A, et al. 2015. In situ expression of eukaryotic ice-binding proteins in microbial communities of Arctic and Antarctic sea ice. *ISME J.* 9: 2537–2540.

Verbruggen H, Ashworth M, LoDuca ST, Vlaeminck C, Cocquyt E, et al. 2009. A multi-locus time-calibrated phylogeny of the siphonous green algae. *Mol Phylogenet Evol.* 50: 642–653.

Wu T, Yu L, Zhang Y, Liu J. 2021. Characterization of fatty acid desaturases reveals stress-induced synthesis of C18 unsaturated fatty acids enriched in triacylglycerol in the oleaginous alga *Chromochloris zofingiensis*. *Biotechnol Biofuels.* 14: 184.

Zhang X, Cvetkovska M, Morgan-Kiss R, Huner NPA, Smith DR. 2021a. Draft genome sequence of the Antarctic green alga *Chlamydomonas* sp. UWO241. *iScience.* 24: 102084.

Zhang Z, Qu C, Zhang K, He Y, Zhao X, et al. 2020. Adaptation to extreme Antarctic environments revealed by the genome of a sea ice green alga. *Curr Biol.* 30: 3330–3341.

Zhang Y, Ye Y, Bai F, Liu J. 2021b. The oleaginous astaxanthin-producing alga *Chromochloris zofingiensis*: potential from production to an emerging model for studying lipid metabolism and carotenogenesis. *Biotechnol Biofuels.* 14: 119.